THE JOURNAL OF BIOLOGICAL CHEMISTRY
Vol. 280, No. 13, Issue of April 1, pp. 12069–12076, 2005

Printed in U.S.A.

Jingzhaotoxin-I, a Novel Spider Neurotoxin Preferentially Inhibiting Cardiac Sodium Channel Inactivation*

Received for publication, October 13, 2004, and in revised form, November 9, 2004
Published, JBC Papers in Press, November 17, 2004, DOI 10.1074/jbc.M411651200

Yucheng Xiao‡, Jianzhou Tang‡, Weijun Hu‡, Jinyun Xie‡, Chantal Maertens§‖, Jan Tytgat§, and Songping Liang‡¶

From ‡College of Life Sciences, Hunan Normal University, Changsha 410081, China and §Laboratory of Toxicology, University of Leuven, E. Van Evenstraat 4, 3000 Leuven, Belgium

Jingzhaotoxin-I (JZTX-I), a 33-residue polypeptide, is derived from the Chinese tarantula *Chilobrachys jingzhao* venom based on its ability to evidently increase the strength and the rate of vertebrate heartbeats. The toxin has three disulfide bonds with the linkage of I-IV, II-V, and III-VI that is a typical pattern found in inhibitor cystine knot molecules. Its cDNA determined by rapid amplification of 3′- and 5′-cDNA ends encoded a 62-residue precursor with a small proregion of eight residues. Whole-cell configuration indicated that JZTX-I was a novel neurotoxin preferentially inhibiting cardiac sodium channel inactivation by binding to receptor site 3. Although JZTX-I also exhibits the interaction with channel isoforms expressing in mammalian and insect sensory neurons, its affinity for tetrodotoxin-resistant subtype in mammalian cardiac myocytes (IC_{50} = 31.6 nM) is ~30-fold higher than that for tetrodotoxin-sensitive subtypes in latter tissues. Not affecting outward delay-rectified potassium channels expressed in *Xenopus laevis* oocytes and tetrodotoxin-resistant sodium channels in mammal sensory neurons, JZTX-I hopefully represents a potent ligand to discriminate cardiac sodium channels from neuronal tetrodotoxin-resistant isoforms. Furthermore, different from any reported spider toxins, the toxin neither modifies the current-voltage relationships nor shifts the steady-state inactivation of sodium channels. Therefore, JZTX-I defines a new subclass of spider sodium channel toxins. JZTX-I is an α-like toxin first reported from spider venoms. The result provides an important witness for a convergent functional evolution between spider and other animal venoms.

Voltage-gated sodium channels (VGSCs)[1] are integral plasma membrane proteins composed of a pore-forming α-subunit (260 kDa) associated with up to four auxiliary β subunits (21–23 kDa) (1, 2). VGSCs play a vital role in the initiation and propagation of exciting signals on most excitable tissues. Similar to the "shaker" potassium channel, the three-dimensional structure of sodium channel is a bell-shaped molecule (3, 4). From mammals, over ten mammalian subtypes ($Na_v1.1$–1.9 and Na_vx) exhibiting relatively similar pharmacological properties in different expression systems have been identified and characterized. Sequence analysis demonstrates that they have been highly conserved during evolution. Furthermore, to be beneficial for catching their prey, the properties of sodium channels in many animals even have evolved geographically in a coevolutionary arms race with their toxic prey (5, 6).

Many polypeptides targeting VGSCs have been identified in many kinds of animal venoms, such as those from scorpions, spiders, snakes, and marine animals. With different critical residues and distinct functional characterization, these naturally occurring toxins are proved to be important tools in distinguishing the different subtypes and disclose the function-structure relationships of VGSCs. Over six neuronal receptor sites are suggested to elucidate such relationships (7). Based on the analysis of precursor organization and gene structure combined with a three-dimensional fold, Zhu *et al.* (8) suggest that inhibitor cystine knot (ICK) peptides from animals shared a common evolutionary origin. Compared with scorpion and snake toxins, spider peptides are shorter ones containing around 35 residues with three/four disulfide bonds. Despite distinct amino acid compositions, most spider peptides have also been found to share a clear homological ICK fold determined structurally by NMR and homology modeling techniques (9). The majority of them such as δ-atracotoxins (δ-ACTXs) and μ-agatoxins share a common mode of inhibiting inactivation kinetics of sodium currents on vertebrate or/and insect VGSCs by binding to receptor site 3 (10–12). Functional convergence widely occurs among animal toxins with different origins during evolution (8, 14). Many significant evidences appear in scorpions, snakes, and marine animals, but similar evidence still remains to be found in spiders. The remarkable functional difference between spider site-3 toxins and other animal toxins is that spider site 3 toxins evidently depress current amplitudes, whereas other animal toxins enhance current amplitudes evoked under whole-cell patch clamp recording (10–12). Spider site 3 toxins show no effects on tetrodotoxin-resistant (TTX-R) sodium channels such as $Na_v1.5$ and $Na_v1.8$–1.9. New emerging ligands will play an important role in elucidating their subtle difference. Moreover, they have been proven to be potential valuable pharmaceutics or insecticides (13).

Here we report the isolation, cDNA sequence determination, and functional characterization of a novel sodium channel toxin, Jingzhaotoxin-I (JZTX-I), from the venom of Chinese tarantula *Chilobrachys jingzhao* (*Araneae*:*Theraphosidae*:*Chi-*

* This work was supported by National Natural Science Foundation of China under contract number 30430170 and by Grant G.0081.02 (to F. W. O.-Vlaanderen). The costs of publication of this article were defrayed in part by the payment of page charges. This article must therefore be hereby marked "*advertisement*" in accordance with 18 U.S.C. Section 1734 solely to indicate this fact.

¶ To whom correspondence should be addressed: College of Life Sciences, Hunan Normal University, Changsha 410081, China. Tel.: 86-731-8872556; Fax: 86-731-8861304; E-mail: liangsp@hunnu.edu.cn.

‖ A postdoctoral research fellow (postdoctoral onderzoeker of the Fund for Scientific Research-Flanders (F. W. O.-Vlaanderen).

[1] The abbreviations used are: VGSC, voltage-gated sodium channel; K_v, voltage-gated potassium channel; TTX, tetrodotoxin; TTX-R, TTX-resistant; TTX-S, TTX-sensitive; DRG, dorsal root ganglion; RACE, rapid amplification of cDNA ends; ICK, inhibitor cystine knot; HPLC, high pressure liquid chromatography; MALDI-TOF, matrix-assisted laser desorption/ionization time-of-flight; TCEP, Tris-(2-carboxyethyl)phosphine; HNTX, Hainantoxin.

lobrachys) (15). The toxin is composed of 33 residues stabilized by three disulfide bridges (I-IV, II-V, and III-VI) assigned by partial reduction, sequencing, and multi-enzymatic digestion. JZTX-I shows no effect on neuronal TTX-R VGSCs and K_v1 channels, but it inhibits channel inactivation of neuronal TTX-S subtypes and cardiac TTX-R subtypes. To the best of our knowledge, JZTX-I is an α-like toxin first reported to date from spider venoms. It provides an important witness for studying the convergent and divergent functional evolution of animal venoms.

EXPERIMENTAL PROCEDURES

Toxin Purification and Sequencing—JZTX-I was fractionated from Chinese tarantula *C. jingzhao* venom using a combination of ion-exchange chromatography and reverse-phase high pressure liquid chromatography (HPLC) as previous described (13). Lyophilized venom (10 mg in 2 ml in distilled water) was applied to a Waters protein-Pak CM 8 H column (5 × 50 mm) initially equilibrated with 0.2 M sodium phosphate buffer, pH 6.25 (buffer A). The column then was eluted with a linear gradient (see Fig. 1*A*) at a flow rate of 3.0 ml/min. The fraction of interest collected was applied to a Vydac C18 (C4) analytical reverse-phase HPLC column (218TP54, 4.6 × 250 mm) and eluted at a flow rate of 0.7 ml/min by a linear gradient of acetonitrile containing 0.1% v/v trifluoroacetic acid (see Fig. 1*B*). The molecular mass and purity of toxin were determined by matrix-assisted laser desorption/ionization time-of-flight (MALDI-TOF) mass spectrometry. The full amino acid sequence (Swiss-Prot accession numbers P83974 and AJ854060) was obtained from a single sequencing run on an Applied Procise™ 491-A protein sequencer by automated Edman degradation.

Assignment of the Disulfide Bridges of JZTX-I—Native peptide (0.1 mg) was partially reduced in 20 μl of citrate buffer (1 M, pH 3.0) containing 6 M guanidine-HCl and 0.05 M Tris (2-carboxyethyl)phosphine (TCEP) at 40 °C for 10 min. The fractions monitored at 280 nm were separated on a C18 reverse-phase HPLC column with a linear gradient elution (25–50% acetonitrile in 40 min). The masses of all of the fractions collected were determined by MALDI-TOF mass spectrometry. The intermediate with free thiols were lyophilized and then alkalized by adding 100 μl of 0.5 M iodoacetamide, pH 8.3. The alkalized peptide was desalted by reverse-phase HPLC and then submitted to an Applied Biosystems Model 491 gas-phase sequencer. The Edman degradation was performed with a normal automatic cycle program. Concerning the protease digestion strategy, native JZTX-I (0.1 mg) was dissolved in 0.2 ml of Tris-HCl (0.2 M, pH 7.5) buffer containing trypsin (4 μg), chymotrypsin (4 μg), and V_8 protease (4 μg). The mixture was incubated at 37 °C for 16 h. The masses of enzymolytic products then were analyzed using MALDI-TOF mass spectrometry.

Identification of JZTX-I cDNA—The full-length of JZTX-I cDNA was obtained using rapid amplification of cDNA ends (RACE) methods as described previously (27). First, according to the manufacturer's instruction, the total RNA was extracted from 0.1 g of fresh venom glands of female spiders using TRIzol reagent kit. 5 μg of RNA was taken to convert mRNA into cDNA using the Superscript II reverse transcriptase with a universal oligo(dT)-containing adapter primer (5′-GGCCACGCGTCGACTAGTAC$(dT)_{17}$-3′). The cDNA then was used as template for PCR amplification in 3′-RACE. Degenerate primer 1 (5′-GC(A/T/C/G)AA(C/T)TT(T/C)GC(A/C/G/T)TG(T/C)AA(G/A)AT(A/C/T)-3′) was designed corresponding to the N-terminal residues (^{18}ANFACKI^{24}) of mature JZTX-I. The partial cDNA of mature toxin was amplified by PCR technique using primer 1. Second, based on the partial cDNA sequence of JZTX-I determined by 3′-RACE, the antisense primers were designed and synthesized for 5′-RACE as gene-specific primer 2 (5′-GGCCTAAGGGCTCCAGATACA-3′). With the strategy described by the RACE kit supplier, the 5′-end cDNA of JZTX-I was amplified using its gene-specific primer 2. Amplified products in both 3′- and 5′-RACE were precipitated and cloned into the pGEM-Teasy vector for sequencing. DNA sequencing was performed by Bioasia Inc. Nucleic acid sequences were analyzed using the software of DNAclub (by Xiongfong Chen) and DNAman (by Nynnon Biosoft).

Cell Preparation—Rat DRG neurons were acutely dissociated and maintained in a short-term primary culture according to the procedures adapted from Xiao *et al.* (16). 30-day-old adult Sprague-Dawley rats of either sex, in adherence with protocols approved by the Hunan Normal University Animal Care and Use Committee, were killed by decapitation without anesthetization, the dorsal root ganglia were removed quickly from the spinal cord, and then they were transferred into Dulbecco's modified Eagle's medium containing trypsin (0.5 g/liter, type III), collagenase (1.0 g/liter, type IA), and DNase (0.1 g/liter, type III) to incubate at 34 °C for 30 min. Trypsin inhibitor (1.5 g/liter, type II-S) was used to terminate enzyme treatment. The DRG cells were transferred into 35-mm culture dishes (Corning, Sigma) containing 95% Dulbecco's modified Eagle's medium, 5% newborn calf serum, hypoxanthine aminopterin thymidine supplement, and penicillin-streptomycin and then incubated in the CO_2 incubator (5% CO_2, 95% air, 37 °C) for 1–4 h before the patch clamp experiment.

Single ventricular cardiomyocytes were enzymatically dissociated from adult rats according to the procedures adapted from Xiao and Liang (17). Sprague-Dawley rats (~250 g) of either sex were killed by decapitation without anesthetization, and the heart was rapidly removed and rinsed in ice-cold Tyrode's solution containing (in mM): 143.0 NaCl; 5.4 KCl; 0.3 NaH_2PO4; 0.5 $MgCl_2$; 10.0 glucose; 5.0 HEPES; and 1.8 $CaCl_2$ at pH 7.2. The heart then was mounted on a Langendorff apparatus for retrograde perfusion via the aorta with non-recirculating Ca^{2+}-free Tyrode's solution bubbled at 37 °C by 95% O_2 and 5% CO_2. After 10 min, perfusate was switched to a Ca^{2+}-free Tyrode's solution supplemented with 0.3% collagenase IA and 0.7% bovine serum albumin and the hearts were perfused in a recirculated mode for 5 min. After the enzymatic solution was replaced by KB buffer ((in mM) 70.0 L-glutanic; 25.0 KCl; 20.0 taurine; 10.0 KH_2PO_4; 3 $MgCl_2$; 0.5 EGTA; 10.0 glucose; and 10.0 HEPES at pH 7.4), the partially digested hearts were cut, minced, and gently triturated with a pipette in the KB buffer at 37 °C for 10 min. The single cells were obtained after undigested tissues filtered through a 200-μm nylon mesh. All of the cells were used within 8 h of isolation.

Cotton bollworm central nerve ganglion neurons were acutely dissociated and maintained in a short-term primary culture as described previously (18). 10-day-old cotton bollworms were killed in 75% alcohol and washed in saline containing the following (in mM): 90 NaCl; 6 KCl; 2 $MgCl_2$; 10 HEPES; and 140 D-glucose at pH 6.6. After being wiped off the enteron, the central nerve ganglia were removed quickly. The nerve ganglia torn then were incubated at room temperature (20–25 °C) in enzyme solution for 20 min containing the following: 90 mM NaCl; 6 mM KCl; 10 mM HEPES; 25 mM D-glucose; 115 mM D-mannitol; 0.3% trypsin; and 0.15% collagenase IV at pH 6.6. Their enzymatic digestion was stopped in 35-mm-culture dishes containing 45% TC-100 (Invitrogen), 45% Dulbecco's modified Eagle's medium (Sigma), 10% fetal bovine serum, 100 mM D-glucose, 0.6 mM glutamine, glutathione, and penicillin-streptomycin at pH 6.6. After the cells in the ganglia were gently dispersed using a suction tube, they were incubated in CO_2 incubator (5% CO_2, 95% air, 28 °C) for 2–3 h before the patch clamp experiment.

Whole-cell Recording—Sodium currents were recorded from experimental cells using whole-cell patch clamp technique at room temperature (22–25 °C). Recording pipettes (2–3 μm in diameter) were made from borosilicate glass capillary tubing, and its resistances were 1.0–2.0 megohms when filled with internal solution contained the following (in mM): 135 CsF; 10 NaCl; and 5 HEPES at pH 7.0. The external bathing solution contained the following (in mM): 30 NaCl; 5 CsCl; 25 D-glucose; 1 $MgCl_2$; 1.8 $CaCl_2$; 5 HEPES; 20 triethanolamine chloride; and 70 tetramethylammonium chloride at pH 7.4. After establishing the whole-cell recording configuration, the resting potential was held at −80 mV for at least 4 min to allow adequate equilibration between the micropipette solution and the cell interior. Ionic currents were filtered at 10 kHz and sampled at 3 kHz on EPC-9/10 patch clamp amplifier (HEKA, Lambrecht, Germany). The P/4 protocol was used to subtract linear capacitive and leakage currents. Experimental data were acquired and analyzed by the program Pulse+Pulsefit8.0 (HEKA). The needed concentrations of toxin dissolved in external solution were applied onto the surface of experimental cells by low-pressure injection with a microinjector (IM-5B, Narishige). Concerning DRG neurons containing TTX-S and TTX-R sodium channels, the cells with diameters of 30–40 μm were chosen for the experiments. Larger DRG cells (>30 μm) tended to express TTX-S VGSCs, whereas the smaller ones (<10 μm) tended to express TTX-R VGSCs (19). TTX-R currents were separated from total currents using 0.2 μM TTX blocking TTX-S channels completely.

Evolutionary Tree of Spider Sodium Channel Toxins—The phylogeny of spider sodium channel toxins was constructed as described previously (14). In our study, we focused on the spider toxins from the species in the family *Mygalomorphae*. Two groups of well known spider toxins (μ-agatoxin I-VI and δ-paluIT 1–4) were chosen as typical representations of the family *Araneomorphae* to outline the phylogeny clearly (12, 20). Multiple sequences of spider toxins were edited using the Bioedit Sequence Alignment Editor software and then aligned and refined manually using ClustalW1.8 program (21). A pairwise distance matrix was calculated on the basis of the proportions of different amino acids.

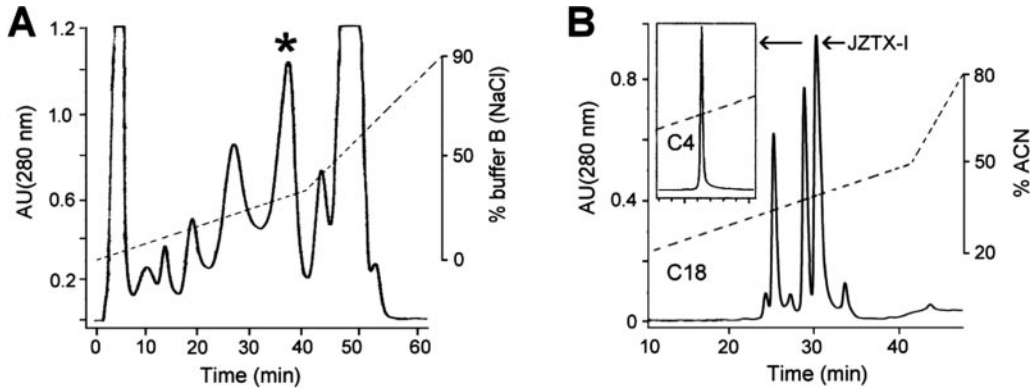

FIG. 1. **Purification and identification of JZTX-I.** *A*, ion-exchange HPLC chromatograph of the crude venom. An *asterisk* indicated the fraction with the retention time of 47.3 min containing the component of interest. *B*, analytical reverse-phase HPLC profile of the interest fraction on C18/C4 column. The linear gradients of buffer B (NaCl or acetonitrile (*ACN*)) were indicated with a *dashed line* in *A* and *B*. *AU*, arbitrary units.

The matrix was then used to construct trees by the neighbor-joining method (MEGA2.1) (22). The reliability of branching patterns was assessed using 1000 bootstrap replications.

RESULTS

Purification and Sequence Analysis of JZTX-I—The fraction of interest (JZTX-I) was purified using a combination method of ion-exchange HPLC and reverse-phase HPLC (Fig. 1) based on its ability to evidently increase the strength and the rate of vertebrate heartbeats (figure not shown). The molecular mass of naturally occurring toxin was determined to be 3675.64 Da by MALDI-TOF mass spectrometry. Its full amino acid sequence was performed by N-terminal Edman degradation and found to be composed of 33 residues including six cysteines (Fig. 3*A*). Six cysteines were assayed to form three disulfide bridges by the molecular mass of alkalized sample, which increased 58 × 6 Da. The calculated molecular mass (3675.4 Da) corresponding to the primary sequence was consistent with the measured mass, suggesting that the C-terminal residue (Pro^{33}) was not amidated. JZTX-I was a novel tarantula toxin exhibiting limited sequence similarity with any reported peptide but 50.0% with JZTX-III. Despite the significant sequence divergence, sequence alignment indicated that all six cysteines in JZTX-I were strictly conserved at similar positions in most spider peptides adopting a typical ICK fold such as HWTX-I, ProTx-I, and HNTX-I.

Assignment of the Disulfide Bridges of JZTX-I—Fig. 2*A* showed the typical reverse-phase HPLC separation of the partially reduced mixture of JZTX-I by TECP. As MALDI-TOF mass spectrometry analysis pointed out, only one intermediate was obtained and further resolved to contain one disulfide bridge in peak II, whereas peaks I and III represented intact peptide and completely reduced peptide, respectively, because their molecular masses increased by 0 (peak I), 4 (peak II), and 6 Da (peak III) compared with that of native peptide, respectively. Peak II then was collected and alkalized immediately with iodoacetamide followed by further purification using reverse-phase HPLC. Molecular mass determination and sequencing indicated that the free thiols of the fraction of interest had been alkylated. The sequencing results showed that the signals of Pth-CM-Cys signals were observed except at the 16th and 29th cycles, positively supporting that the remaining disulfide bridge was cross-linked by Cys^{16}-Cys^{29}. In Fig. 2*B*, when JZTX-I was exposed to multi-enzymes (trypsin, chromotrypsin, and V_8 protease) in the buffering solution, a series of smaller enzymolytic fragments was produced and their molecular masses were measured by MALDI-TOF mass spectrometry. The reverse-phase HPLC separation of the enzymolytic mixture could produce a 2176-Da fragment, which was sequenced to be Ala^1-Trp^6 (containing Cys^2), Gly^{12}-Phe^{20} (Cys^{16} and Cys^{17}), and Leu^{28}-Trp^{31} (Cys^{29}), as described in Fig. 2*B*, *inset*. Thus two disulfide bridges should be paired among Cys^2, Cys^{16}, Cys^{17}, and Cys^{29}. Because a disulfide bridge between Cys^{16} and Cys^{29} had been determined above, we concluded that the second was cross-linked between Cys^2 and Cys^{17}. Accordingly, by process of elimination, the third disulfide bond was between Cys^9 and Cys^{22}.

Therefore, the disulfide linkage of JZTX-I was homologous to that for ICK peptides from spider venoms, such as ProTxs, HWTX-IV, and HNTX-I, as well as conotoxins (δ-, μ-, κ-, and ω-), although the positions of six cysteines were not conserved between them (13, 23–25).

Cloning and Sequencing JZTX-I cDNA—The full-length cDNA sequence of JZTX-I was completed by overlaying two fragments resulting from 3′- and 5′-RACE. As shown in Fig. 3*B*, the oligonucleotide sequence of the cDNA was a 383-bp bond found to comprise a 5′-untranslated region, open reading frame, and 3′-untranslated region. The open reading frame encoded a 63-residue peptide (Swiss-Prot accession number AJ854060) corresponding to the JZTX-I precursor that contained a signal peptide of 21 residues, a propeptide of 8 residues, and a mature peptide of 33 residues. The pre-proregion composed of a signal peptide and a propeptide is a hydrophobic peptide common to all spider toxins. Furthermore, its homology is important proof that spider toxins can be grouped into different superfamilies to analyze their evolutionary relationship. The pre-propeptide of JZTX-I precursor showed limited sequence identity with that of other reported precursors but 66.7 and 57.1% with JZTX-III and GsMTx-4 (16, 26), respectively. Different from most spider sodium channel toxins, JZTX-I had no extra amino acid residues Gly or (Gly + Arg/Lys) at its C terminus known to allow "post-modification" and α-amidation at the C-terminal residue (27), also implying that the C-terminal residue of mature toxin is not amidated. A polyadenylation signal (AATAAA) emerged in the 3′-untranslated region at position 17 upstream of the poly(A).

Effects of JZTX-I on Sodium Currents—TTX-S and TTX-R VGSCs co-express in adult rat DRG neurons (1), whereas only TTX-S type is distributed in cotton bollworm central nerve ganglion neurons (18). TTX-R VGSCs are the primary type in adult rat ventricular myocytes, although Maier *et al.* (28) suggest that some brain TTX-S subtypes are situated in its transverse tubules (28). The sodium channels expressing in these tissues have been defined as different isoforms based on their divergent amino acid sequences. Generally, TTX-R sodium currents activated and inactivated more slowly than TTX-S types under whole-cell configuration. JZTX-I at 1 μM in the bath solution was resistant to control TTX-R sodium currents in rat DRG neurons (Fig. 4*A*, n = 5) but sensitive to TTX-R currents in ventricular myocytes and

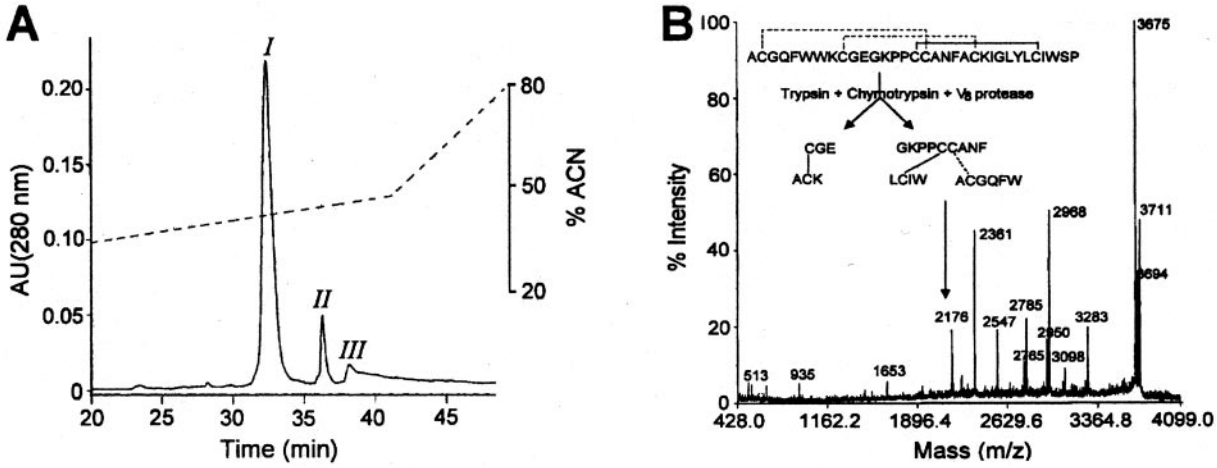

FIG. 2. **Identification of the disulfide bridge pattern of JZTX-I.** *A*, partial reduction of JZTX-I by TCEP was fractionated by reverse-phase HPLC. Three chromatographic peaks contained intact peptide (labeled *I*), partial reduced intermediate (labeled *II*), and complete reduced peptide (labeled *III*), respectively. *ACN*, acetonitrile; *AU*, arbitrary units. *B*, MALDI-TOF mass spectrometry analysis of multi-enzymatic peptide by trypsin, V_8 protease, and chymotrypsin. A fragment with the mass of 2176 Da was chosen to be sequenced as detailed in the *inset* in which the *solid line* indicated the disulfide bridge pair determined by TCEP, whereas *dashed lines* were the undetermined disulfide bridge pairs.

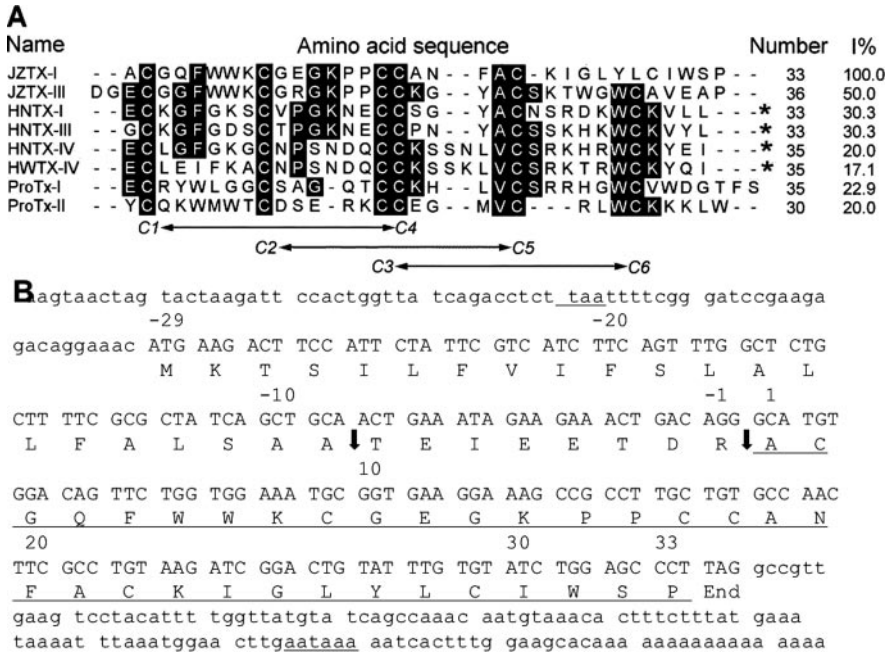

FIG. 3. **Amino acid sequence and cDNA sequence of JZTX-I.** *A*, comparison of the amino acid sequences of seven sodium channel toxins from tarantula venoms. JZTX-I and JZTX-III were isolated from *Chilobrachys jingzhao* (15, 16), ProTx-I and ProTx-II were from *Thrixopelma pruriens* (23), HNTX-I and HNTX-IV were from *Ornithoctonus hainana* (24, 32), and HWTX-IV was from *Ornithoctorus huwena* (13). The toxins had an amidated C terminus indicated with an *asterisk*. The identical residues are shaded in *black*. The conserved disulfide bridge pattern of these toxins is indicated under their sequences. *B*, the oligonucleotide sequence of JZTX-I cDNA. The amino acid composition of the precursor reading from the cDNA is suggested below the nucleotide sequence. The potential endoproteolytic sites are pointed out with *down arrows*. The sequence of mature peptide is *underlined* by a *solid line*.

TTX-S currents in sensory neurons (Fig. 4, *B–D*). JZTX-I evidently inhibited channel inactivation with distinct affinity on three tested tissues without changing peak current amplitudes or the time of current peak. A similar result was detected after the application of β-pompilidotoxin, which was considered to selectively interfere with sodium channel inactivation process without affecting the activation (29). The efficiency of the toxin then was assayed by measuring the $I_{5\ ms}/I_{peak}$ ratio, which gave an estimate of the probability for the channel not to be inactivated after 5 ms. JZTX-I at 1 μM inhibited channel inactivation of TTX-S currents in rat DRG neurons by 51.2 ± 8.0% (Fig. 4*B*, $n = 20$), whereas an equal inhibition of TTX-R currents was achieved in rat cardiac myocytes exposed to the toxin only at 50 nM (Fig. 4*C*, $n = 5$). The toxin at 1 μM could slow the decay of TTX-S sodium currents in cotton bollworm neurons by 52.4 ± 6.8% (Fig. 4*D*, $n = 11$). All of the inhibitions above were in a time-dependent and concentration-dependent manner, and their IC_{50} values were assessed to be 0.13 μM, 31.6 nM, and 0.76 μM, respectively (Fig. 4*E*). Furthermore, we checked the ion component of the inward currents maintained at the ending of depolarizing pulse. Because they could be eliminated in both rat DRG and insect neurons by TTX (0.2 μM) completely in Fig. 4*B* ($n = 8$), ion currents were still conducted through sodium channels. The fact demonstrated that JZTX-I did not change the ion selectivity of sodium channels.

Fig. 5 showed the families of superimposed sodium currents in rat DRG neurons, rat cardiac myocytes, and cotton bollworm neurons. The control current-voltage relationships indicated that their profound properties corresponding to divergent sequences of α-subunit represented some subtle differences in the thresholds of initial activation and the reverse potentials. After ~2 min of JZTX-I application, re-examination revealed that inhibiting channel inactivation was detected on three tested tissues at the given depolarizing pulses between the threshold and reverse potentials. Interestingly, differing greatly from both spider excitatory toxins (*e.g.* δ-ACTXs) and depressant toxins (*e.g.* HWTX-IV), the novel toxin neither shifted the current-voltage relationships nor changed control peak currents amplitudes (11, 13).

Previous studies have suggested that parallel to inhibiting inactivation kinetics, spider toxins also shifted the steady-state

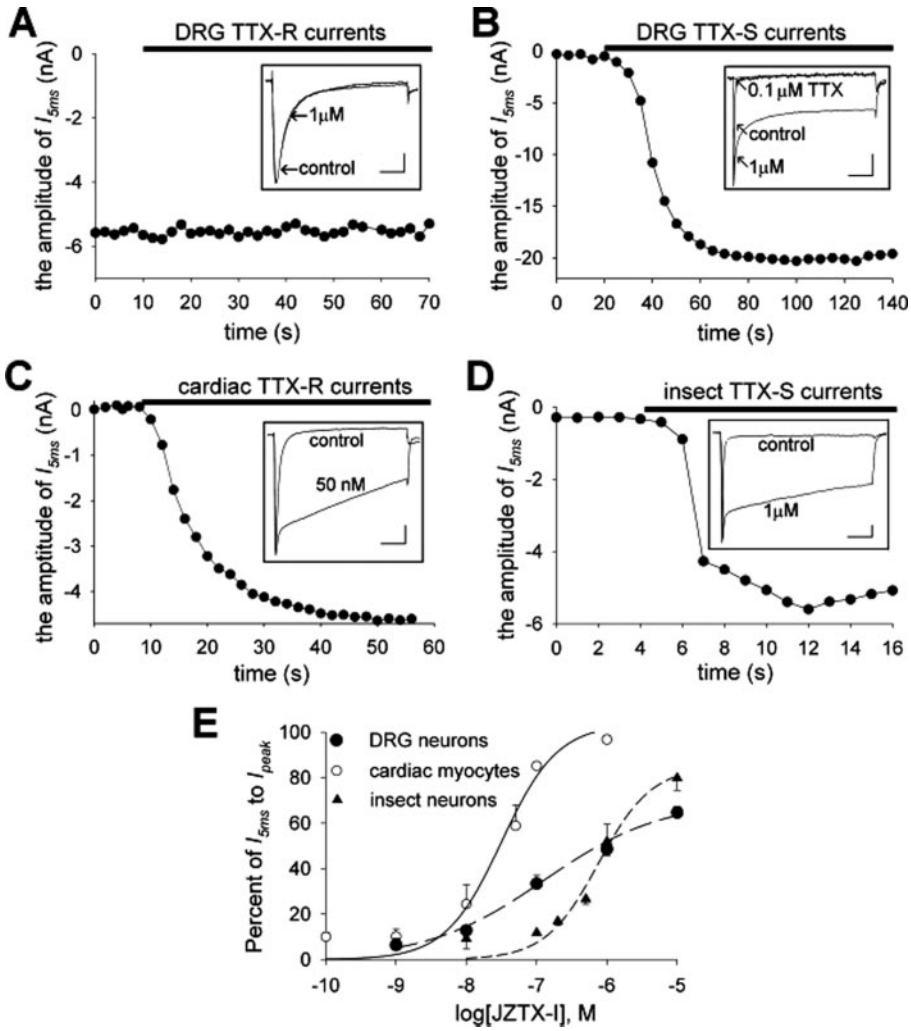

FIG. 4. **Effects of JZTX-I on TTX-S and TTX-R sodium currents.** All of the current traces were elicited by a 50-ms depolarizing potential of −10 mV from a holding potential of −80 mV. *A*—*D*, represented the typical time-dependent inactivation inhibition of JZTX-I on TTX-R currents and TTX-S currents in rat DRG neurons, TTX-R currents in rat cardiac myocytes, and TTX-S currents in cotton bollworm neurons, respectively. The remaining currents at the end of depolarizing pulse could be further blocked by 200 nM TTX completely. JZTX-I at different concentrations failed to change the amplitudes of peak currents recorded in three checked tissues. *E*, the concentration-dependent inhibition of sodium channel inactivation by JZTX-I. Every point (mean ± S.E.) comes from 3–20 separated experimental cells. These points were fitted according to Boltzmann equation, Inhibition% = 100/[1 + exp(C− C_{50})k], where IC_{50} was the concentration of JZTX-I at half-maximal inhibition, k was the slope factor, and C was the concentration of JZTX-I.

inactivation of sodium channels to a more negative potential (11, 17). To further assess the profound actions of JZTX-I on sodium channels, we also investigated the effect of the tarantula toxin on steady-state inactivation by employing a standard two-pulse protocol detailed in the illustration of Fig. 6. Under control condition, the putative midpoint of steady-state inactivation was around −57.1 mV in adult rat DRG neurons and cardiac myocytes, whereas it was −39.1 mV in cotton bollworm neurons. Unexpectedly, JZTX-I treatment did not evidently shift the steady-state inactivation in three experimental tissues, although channel inactivation inhibition remained at test pulses similar to other spider excitatory toxins (*e.g.* δ-ACTXs) (10, 11).

Effects of JZTX-I on Voltage-gated Potassium Channels—Spider venoms contain many potassium channel toxins with high affinity besides sodium channel toxins. Although they are known to be potent specific for their respective receptors, Middleton *et al.* (23) reported ProTx-I at <1 μM, a sodium channel toxins from the tarantula *Therixopelma pruriens* venom, also partially blocked K_v1.2 channel expressed in oocytes (23). Here we further checked the toxin on three different voltage-gated potassium channels isoforms (K_v1.1–1.3 channel) expressed in *Xenopus laevis* oocytes using the two-electrode voltage clamp technique (30). However, no effects were detected after application of JZTX-I at 1 μM (Fig. 7).

DISCUSSION

Sodium channel toxins from venomous animals have been shown to lead to new insecticides and pharmaceuticals. To elucidate, their structure-function relationship enhances our understanding of the properties of sodium channel proteins. In this work, we have isolated and characterized a novel spider toxin, JZTX-I, from the Chinese tarantula *C. jingzhao* venom (15). Containing a conserved disulfide connectivity (I-IV, II-V, and III-VI) and conforming exactly to the ICK definition as described by Escoubas *et al.* (31), JZTX-I represents a typical ICK structure, although it exhibits significant sequence divergence with other ICK peptides (24, 32). JZTX-I is a preferential cardiac sodium channel neurotoxin (IC_{50} = 31.6 nM) not affecting K_v1.1–1.3 channels and neuronal TTX-R VGSCs. Its potential modulating site is reasonably assumed to receptor site 3.

The general biochemical features of JZTX-I precursor read from the cDNA sequence are similar to most spider toxin precursors that are predicted to comprise a signal peptide, an intervening propeptide, and a mature peptide (8, 27). The structural organization suggests that JZTX-I should be matured through a post-translational cleavage during the course of secretion where the pre-propeptide can be removed at an endroproteolytic site anterior to mature peptide. Different from JZTX-III precursor having an uncommon signal site (-*X*-Ser-) (16), JZTX-I precursor contains one site (-*X*-Arg-) common to most animal toxin precursors. Generally, the similarities of the pre-propeptide sequences are important criteria for defining the superfamilies for naturally occurring toxins. The toxins in the same superfamily always share conserved regions in the pre-proregion, particularly in the signal peptide. Because their pre-propeptides exhibit a 51.7% sequence identity with each

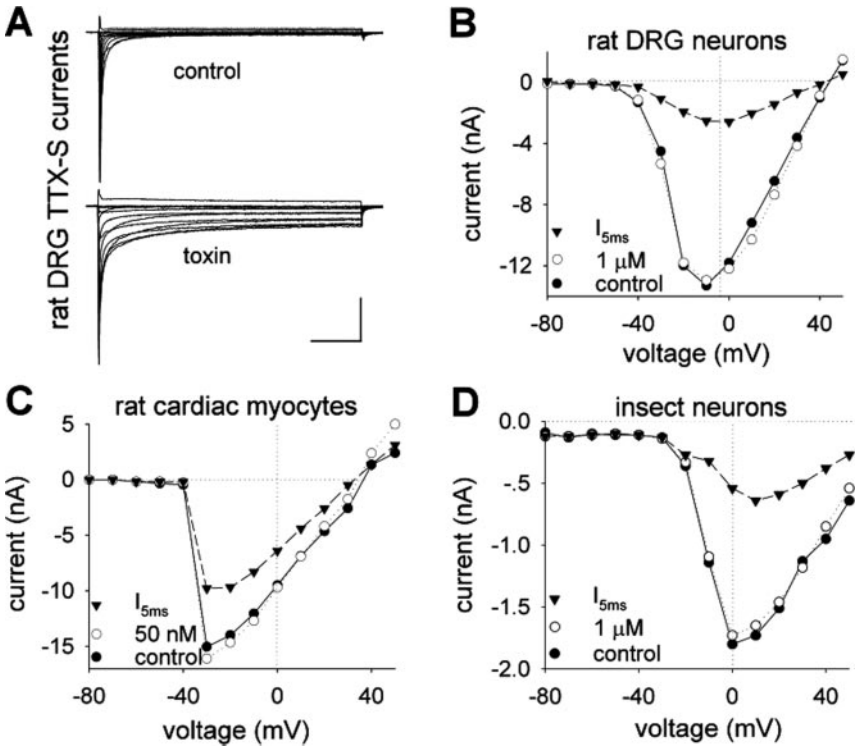

FIG. 5. **Effects of JZTX-I on the current-voltage relationships of sodium channels.** The family of both TTX-S and TTX-R current traces were induced by 50-ms depolarizing steps to various potentials from a holding potential of −80 mV. Test pulses ranged from −80 to +50 mV. The I-V curves showed the relationships between current traces before (control) and after adding JZTX-I at different concentrations in rat DRG neurons (*A* and *B*), rat cardiac myocytes (*C*), and cotton bollworm neurons (*D*), respectively. In *B–D*, $I_{5\ ms}$ was shown as the current inactivated at 5 ms.

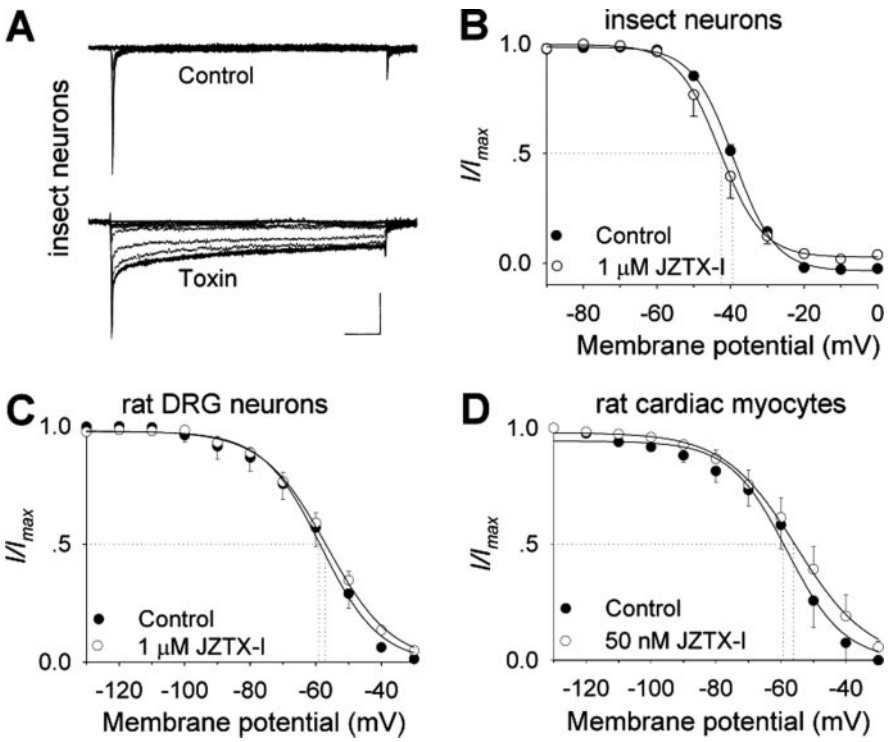

FIG. 6. **Effects of JZTX-I on the steady-state inactivation of sodium channels.** In cotton bollworm neurons *A* and *B*, sodium currents were induced by a 50-ms depolarizing potential of +20 mV for various prepulse potentials for 1 s ranging from −90 to 0 mV. In rat DRG neurons (*C*) and cardiac myocytes (*D*), sodium currents were induced by a 50-ms depolarizing potential of −10 mV from various prepulse potentials for 1 s that ranged from −130 to −30 mV with a 10-mV increment. The data dots shown as the ratio of I_{test} to I_{max} were fitted according to the Boltzmann equation, $I_{test}/I_{max} = 1/(1 + \exp((V - V_{½})/k))$, where V was the prepulse potential, $V_{½}$ pointed out further by *dashed lines* was the voltage at which I was 0.5 I_{max}, and k was the slope factor. After the treatment of JZTX-I at 1 μM, 50 nM, and 1 μM, the $V_{½}$ values were shifted only by +2.0 mV (−59.0 → −57.0 mV), +2.8 mV (−55.3 → −58.1 mV), and −3.7 mV (−39.1 → −42.8 mV) in rat DRG neurons, cardiac myocytes, and cotton bollworm neurons, respectively.

other, JZTX-I should belong to the same superfamily as JZTX-III in the tarantula *C. jingzhao*. Interestingly, further analysis indicated that the proregion length in both JZTX-I (eight residues) and JZTX-III (five residues) precursors are much smaller than the lengths (over 25 residues) in other cDNAs of spider toxins.

Animal toxins can produce a common evolutionary event in order to be beneficial for catching their prey and defending against their predators (34). An analysis of evolution not only exhibits the evolutionary trace of animal toxins but also can predict their profound functional characterizations. Here we exhibit the phylogeny of spider sodium channel toxins based on their amino acid sequences. As shown in Fig. 8, spider sodium channel toxins are divergent in two evolutionary routes. The tarantula toxins from the family *Theraphosidae* with large body size are clustered in the second branch and preferentially inhibit mammalian sodium channels, whereas the toxins from the family *Hexathelidae* with small body size are clustered into the first branch, suggesting that they derive from different ancestor peptides. Interestingly, our studies also suggested clearly that the ancestor peptides for *Araneomorphae* toxins (δ-paluITs and μ-agatoxins) are more closely related to *Hexathelidae* toxins than

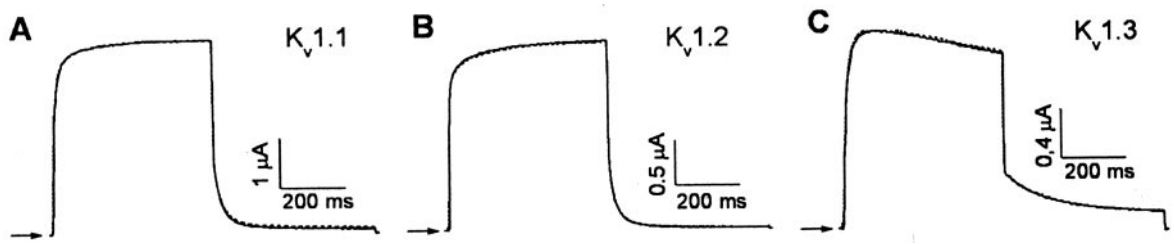

FIG. 7. **Effects of JZTX-I on VGPCs expressed in *Xenopus laevis* oocytes.** K_v1.1 (*A*), K_v1.2 (*B*), and K_v1.3 (*C*) current traces were evoked by a 500-ms depolarization to 0 mV from a holding potential of −90 mV. The tail potential was −50 mV. No evident changes of the currents were detected in the absence (*solid line*) and presence (*dashed line*) of 1 μM JZTX-I (n = 3–5 for each of the clones). *Arrow* indicates zero current level.

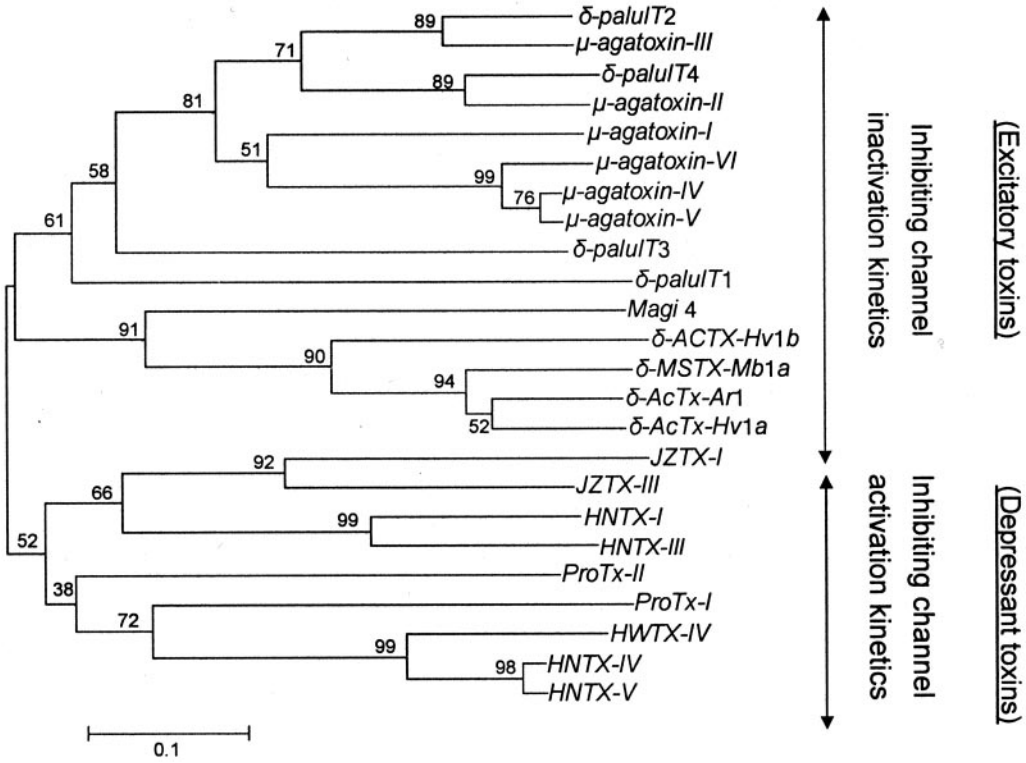

FIG. 8. **Unrooted phylogenetic tree of spider sodium channel toxins.** The numbers on the branches were the bootstrap percentages supporting a given partition. The main characteristic functions of these spider toxins are shown on the *right*.

TABLE I

Analysis of amino acid sequences of receptor site 3 on different sodium channel subtypes

The emerging positions of functional residues are shaded in gray.

		DIV-S3 Extracellular loop DIV-S4
(DRG neuron) TTX-S	Na_v1	SIVGMFLAELIE--KYFVSPTLFRVIRLAR
(skeletal muscle)	$Na_v1.4$	SIVGLALSDLIQ--KYFVSPTLFRVIRLAR
(cardiac myocyte)	$Na_v1.5$	SIVGTVLSDIIQ--KYFFSPTLFRVIRLAR
(DRG neuron) TTX-R	$Na_v1.8$	SIGSLLFSAILKSLENYFSPTLFRVIRLAR
(DRG neuron) TTX-R	$Na_v1.9$	SIVSTMISTLENQEHIPFPPTLFRIVRLAR

to *Theraphosidae* toxins (δ-ACTXs) because they are clustered together in the first branch. The putative suggestion is further supported by the evidence that the disulfide connectivity (I-V, II-VI, III-VII, and IV-VIII) is popular in both of them (35), whereas the disulfide bridge arrangement (I-IV, II-V, and III-VI) is conserved in tarantula toxins (13, 16, 24). JZTX-I from tarantula venom is also clustered in the second branch of the phylogeny. Under whole-cell configuration, the characterizations of JZTX-I on sodium channels are significantly different from those of other tarantula toxins such as HNTXs and ProTxs but similar to those of spider toxins from the species in *Hexathelidae* and *Araneomorphae*. The novel toxin evidently inhibited fast inactivation of TTX-R VGSCs expressed in cardiac myocytes and TTX-S VGSCs expressed in vertebrate and insect sensory neurons and belonged to the excitatory group (32). Intriguingly, unlike δ-ACTXs reducing peak current amplitudes or scorpion α-mammal toxins increasing peak current amplitudes (11, 36), JZTX-I altered the properties of sodium channels in a manner similar to scorpion α-like toxins and β-pompilidotoxin (33, 36). Their treatment shows no any effect on peak current amplitudes, I-V curves, or steady-state inactivation. JZTX-I is an α-like toxin reported first from spider venoms and can define a new subclass

of spider excitatory toxins. It will be important evidence proving the divergent and convergent evolution between spider toxins and other animal toxins.

In the excitatory group, JZTX-I is the unique agent reported to date to alter the properties of $Na_v1.5$ channels. It seems that JZTX-I has the ability to modulate much more VGSC subtypes than other spider toxins. δ-ACTX-Hv1a from Australian funnel-web spider venom is the most famous spider toxin. It inhibits the inactivation of sodium channels in vertebrate and insect sensory neurons (10, 11). However, like other spider excitatory toxins, no similar description has been reported on sodium channels expressed in cardiac myocytes and skeletal muscles. Therefore, JZTX-I hopefully represents a useful ligand to elucidate the common properties among the subtypes of VGSCs and even discriminate $Na_v1.5$ from the other two TTX-R VGSCs ($Na_v1.8$ and $Na_v1.9$). What then is the underlying mechanism for the selectivity? It is well known that receptor site 3 is a short peptide composed of 13–15 residues situated at the Domain IV S3-S4 extracellular loop of the α-subunit protein. Channel determinants demonstrate that three charged residues (Glu^{1613}, Glu^{1616}, and Lys^{1617}), especially Glu^{1613} play a key role in binding peptide toxins. Despite low sequence similarity and different three-dimensional foldings with AaHII (site 3 toxin), three residues (Lys^3, Arg^5, and Asp^{15}) in δ-ACTX-Hv1a were assumed to interact structurally with them, respectively (35). However, the key residues in the depressant group were determined to be Lys^{27} and Arg^{29} located at the loop IV of the HNTX-IV scaffold (32). Such different allocation in two groups of spider toxins may contribute to better match their respective receptor sites. Both Lys^{27} and Arg^{29} are missing in JZTX-I at the corresponding positions; however, three charged residues (Lys^8, Glu^{11}, and Lys^{13}) are also clustered in the putative structure of JZTX-I similar to δ-ACTX-Hv1a (Fig. 3*A*). Further analysis of receptor site 3 indicates that Glu^{1613} and Lys^{1617} in neuronal TTX-S VGSCs are also strictly conserved in cardiac isoforms (Asp^{1612} and Lys^{1616}); however, they are substituted accordingly with uncharged residues (Glu/Asp → Ala/Thr) or anionic residues (Lys → Glu) in neuronal TTX-R subtypes ($Na_v1.8$ and $Na_v1.9$) (see Table I). Moreover, the acidity of Glu^{1613} (pI = 4.6) is weaker than that of Asp^{1612} (pI = 4.3). Rogers *et al.* (37) reported that E1613D significantly increased the affinity of ATX from 76 to 13 nM of the EC_{50}. These facts may partially explain that JZTX-I has a 30-fold affinity with cardiac VGSCs than with neuronal TTX-S isoforms and is preferential to $Na_v1.5$ among three identified TTX-R VGSCs. Because Asp^{1612} in cardiac subtype also conserves in skeletal muscle subtype (see Table I), JZTX-I must be sensitive to $Na_v1.4$. The hypotheses has been supported by the indirect result that the toxin significantly strengthened the normal contractions of mouse diaphragm induced by direct electrical stimulus in which D-tubocurarine at a high concentration was used to block neuromuscular transmission completely.

In summary, in this study, a novel sodium channel toxin has been isolated and characterized from the tarantula *C. jingzhao*. The toxin composed of 33 residues exhibits very low sequence homology with other peptides. It will be a novel useful tool to disclose the structure-functional relationship of receptor site 3 on sodium channel isoforms. Moreover, JZTX-I is the first reported α-like toxin from spider venoms and will contribute to our understanding of the interaction between spiders and other venomous animals during evolution.

Acknowledgments—We thank Olaf Pongs for providing the cDNA for the $K_v1.2$ channel. The $K_v1.3$ clone was kindly provided by Maria L. Garcia. We are grateful to Dr. Bingjun He at Nankai University for technical assistance in the isolation of cotton bollworm central nerve ganglion neurons.

REFERENCES

1. Ogata, N., and Tatebayashi, H. (1993) *J. Physiol.* (*Lond.*) **466,** 9–37
2. Catteral, W. A. (2002) *Neuron* **26,** 13–25
3. Sokolova, O., Kolmakova-Partensky L., and Grigorieff, N. (2001) *Structure* **9,** 215–220
4. Sato, C., Ueno, Y., Asai, K., Takahashi, K., Sato, M., Engel, A., and Fujiyoshi, Y. (2001) *Nature* **409,** 1047–1051
5. Geffeney, S., Brodie, E. D., Jr., Ruben, P. C., and Brodie, E. D., III (2002) *Science* **297,** 1336–1339
6. Huey, R. B., and Moody, W. J. (2002) *Science* **297,** 1289–1290
7. Cestele, S., Ben, Khalifa, R. B., Pelhate, M., Rochat, H., and Gordon, D. (1995) *J. Biol. Chem.* **270,** 15153–15161
8. Zhu, S., Darbon, H., Dyason, K., Verdonck, F., and Tytgat, J. (2003) *FASEB J.* **17,** 1765–1767
9. Shu, Q., Lu, S. Y., Gu, X. C., and Liang, S. P. (2002) *Protein Sci.* **11,** 245–252
10. Grolleau, F., Stankiewicz, M., Birinyi-strachan, L., Wang, X. H., Nicholson, G. M., Pelhate, M., and Lapied, B. (2001) *J. Exp. Biol.* **204,** 711–721
11. Nicholson, G. M., Walsh, R., Little, M. J., and Tyler, M. I. (1998) *Pfluegers Arch. Eur. J. Physiol.* **436,** 117–126
12. Omecinsky, D. O., Holub, K. E., Adams, M. E., and Reily, M. D. (1996) *Biochemistry* **35,** 2836–2844
13. Peng, K., Shu, Q., Liu, Z., and Liang, S. (2002) *J. Biol. Chem.* **49,** 47564–47571
14. Zhu, S., Bosmans, F., and Tytgat, J. (2004) *J. Mol. Evol.* **58,** 145–153
15. Zhu, M. S., Song, D. X., and Li, T. H. (2001) *J. Baoding Teachers College* **14,** 1–6
16. Xiao, Y., Tang, J., Yang, Y., Wang, M., Hu, W., Xie, J., Zeng, X., and Liang, S. (2004) *J. Biol. Chem.* **279,** 26220–26226
17. Xiao, Y. C., and Liang, S. P. (2003) *Eur. J. Pharmacol.* **477,** 1–7
18. He, B. J., Liu, A. X., Chen, J. T., Sun, J. S., Rui, C. H., and Meng, X. Q. (2001) *Acta Entomol. Sin.* **44,** 422–427
19. Su, X., Wachtel, R. E., and Gebhart, G. F. (1997) *Am. J. Physiol.* **277,** 1180–1188
20. Corzo, G., Escoubas, P., Stankiewicz, M., Pelhate, M., Kristensen, C. P., and Nakajima, T. (2000) *Eur. J. Biochem.* **267,** 5783–5795
21. Thompson, J. D., Gibson, T. J., Plewniak, F., Jeanmougin, F., and Higgins, D. G. (1997) *Nucleic Acids Res.* **25,** 4876–4882
22. Saitou, N., and Nei, M. (1987) *Mol. Biol. Evol.* **4,** 406–425
23. Middleton, R. E., Warren, V. A., Kraus, R. L., Hwang, J. C., Liu, C. J., Dai, G., Brochu, R. M., Kohler, M. G., Gao, Y. D., Garsky, V. M., *et al.* (2002) *Biochemistry* **41,** 14734–14747
24. Li, D., Xiao, Y., Hu, W., Xie, J., Bosmans, F., Tytgat, J., and Liang, S. (2004) *FEBS Lett.* **555,** 616–622
25. Shon, K. J., Olivera, B. M., Watkins, M., Jacobsen, R. B., Gray, W. R., Floresca, C. Z., Cruz, L. J., Hillyard, D. R., Brink, A., Terlau, H., and Yoshikami, D. (1998) *J. Neurosci.* **18,** 4473–4481
26. Ostrow, K. L., Mammoser, A., Suchyna, T., Sachs, F., Oswald, R., Kubo, S., Chino, N., and Gottlieb, P. A. (2003) *Toxicon* **42,** 263–274
27. Diao, J. B., Lin, Y., Tang, J. Z., and Liang, S. P. (2003) *Toxicon* **42,** 715–723
28. Maier, S. K., Westenbroek, R. E., Schenkman, K. A., Feigl, E. O., Scheuer, T., and Catterall, A. (2002) *Proc. Natl. Acad. Sci. U. S. A.* **99,** 4073–4078
29. Kinoshita, E., Maejima, H., Yamaoka, K., Konno, K., Kawai, N., Shimizu, E., Yokote, S., Nakayama, H., and Seyama, I. (2001) *Mol. Pharmacol.* **59,** 1457–1463
30. Liman, E. R., Tytgat, J., and Hess, P. (1992) *Neuron* **9,** 861–871
31. Escoubas, P., Diochot, S., and Corzo, G. (2000) *Biochimie* (*Paris*) **82,** 893–907
32. Li, D., Xiao, Y., Xu, X., Xiong, X., Lu, S., Liu, Z., Zhu, Q., Wang, M., Gu, X., and Liang, S. (2004) *J. Biol. Chem.* **279,** 37734–37740
33. Benoit, E., and Gordon, D. (2001) *Neuroscience* **104,** 551–559
34. Froy, O., Sagiv, T., Poreh, M., Urbach, D., Zilberberg, N., and Gurevitz, M. (1999) *J. Mol. Evol.* **48,** 187–196
35. Zeto, T. H., Birinyi-Strachan, L. C., Smith, R., Connor, M., Christie, M. J., King, G. F., and Nicholson, G. M. (2000) *FEBS Lett.* **470,** 293–299
36. Goudet, C., Chi, C. W., and Tytgat, J. (2002) *Toxicon* **40,** 1239–1258
37. Rogers, J. C., Qu, Y., Tanada, T. N., Scheuer, T., and Catterall, W. A. (1996) *J. Biol. Chem.* **271,** 15950–15962